Scientific Journals
Maritime University of Szczecin

Zeszyty Naukowe
Akademia Morska w Szczecinie

2012, 31(103) pp. 128–133

2012, 31(103) s. 128–133

Analysis of a gas turbine used in a high temperature membrane air separation unit

Janusz Kotowicz, Sebastian Michalski

Silesian University of Technology, Institute of Power Engineering and Turbomachinery
44-100 Gliwice, ul. Konarskiego 18, e-mail: janusz.kotowicz@polsl.pl, sebastian.michalski@polsl.pl

Key words: pulverized fuel boiler, oxy-combustion technology, "four end" membrane separator

Abstract

In this article computational algorithm and exemplary results for a model of an air separation unit (ASU) with "four end" high temperature membrane (HTM) were presented. First, the software environment for building of a "four end" membrane separator model was chosen. Then, a model of an air separation unit was created and preliminary calculations were made on that model. The air separation unit structure consists of a "four end" membrane, heat exchanger, electrical generator, air compressor and expander. Parameter that determines all flows in the ASU model is the oxygen mass flow rate. This mass flow rate is approximately the same as oxygen mass flow rate feeding oxy boiler working in a 460 MW power plant. The most important step of this paper was the integration of a model of pulverized fuel boiler in the oxy-combustion technology and the air separation unit model by sending flue gas from boiler to ASU. The characteristics of ASU such as power and efficiency as a function of the oxygen recovery rate were made. Maximal value of oxygen recovery rate was calculated. The difference between optimal compressor pressure ratio of the autonomic gas turbine and of the air separation unit are presented in this paper.

Introduction

Currently appearing world trend to reduce emissions of harmful substances such as greenhouse gases into the environment is changing a direction of the energy technologies [1]. Particularly important is the development of low emission coal technologies that play a significant role in the balance sheets of many countries including Poland, in which a significant part of electricity is generated in coal-fueled power plants. Additionally, during the production of electricity in coal-fueled power plants carbon dioxide emission per produced electricity unit is higher than in other power generation technologies, for example, about 2.5 times more than in gas-steam blocks fueled with natural gas. The two most important directions of research aiming to reduce the emissions from coal-fueled power plants may be mentioned. The first one is the optimization of a power plant within its structure and work parameters. The second direction of development of low emission coal technologies is finding new and optimization of the already known low-energy carbon capture technologies [2]. The currently developed carbon capture technologies are as follows:

- pre-combustion technology;
- post-combustion technology;
- oxy-combustion technology.

Oxy-combustion technology is based on fuel combustion in an atmosphere with increased oxygen concentration in order to eliminate nitrogen from the flue gas. In this technology, flue gas that leaves boiler is composed mainly of carbon dioxide and steam, so the separation of carbon dioxide from flue gas is based on the low energy-consuming condensation process [3, 4]. The oxy-combustion technology is now the most promising solution for carbon energetic technologies [5, 6, 7]. Currently, most advanced is a cryogenic air separation technology. Membrane air separation technologies are also considered, in particular air separation units (ASU) with high temperature membranes (HTM) [8].

Among the currently investigated high-temperature separation membranes, a "three-end" and "four end" membrane-types should be distinguished [9]. The oxygen flow through the membrane is caused by the oxygen partial pressure difference on both sides of a membrane. "four-end" type

membrane used for air separation is immersed on one side by compressed air, while the other side of a membrane is immersed by flue gas from boiler. Oxygen mass flow rate permeating through the membrane depends on a membrane constant (C), oxygen partial pressure on the feed side of the membrane (p_{O2_F}) and oxygen partial pressure on the permeate side (p_{O2_Per}). The relationship between these quantities is expressed by the following formula:

$$j_{O2} = C \cdot \ln\left(\frac{p_{O2\_F}}{p_{O2\_Per}}\right) \ [\text{mol/sm}^2] \qquad (1)$$

The membrane constant (C) in (1) depends, among other, on the thickness of the membrane and the membrane working temperature.

Figure 1 shows a power plant diagram with average integration with air separation unit (ASU) that contains "four end" high temperature membrane for air separation. It should be noted that for the increase of the oxygen partial pressure on the feed side of membrane the compressor with pressure ratio β_K is used. Steam cycle of this power plant is composed of a steam turbine, four low pressure and three high pressure feed-water heaters, condenser, deaerator, condensate pump, feed-water pump, one low-pressure and one high-pressure flue gas-water heat exchangers and one low pressure retentate-water heat exchanger. The steam turbine consist of three parts: high-pressure, intermediate--pressure and low-pressure. Between the intermediate and high-pressure part of the steam turbine steam is reheated. Water heated in steam cycle is directed first to the two parallel economizers and then the water is directed to the boiler. One of the economizers is fed with the flue gas and second with the permeate. Flue gas with the temperature at 850ºC leaving the boiler are subjected to high temperature filtration. Then, part of the flue gas is supplied to the air separation unit. The remaining flue gas is cooled by water and then compressed. The air separation unit is composed of the "four--end" high temperature separation membrane, counter-flow permeate-air heat exchanger, economizer, permeate fan, air compressor, expander and electric generator. The flue gas supplied to ASU is flowing to the separation membrane, where is enriched in oxygen. The gas leaving the membrane (called permeate) heats compressed air in a counter-current permeate-air heat exchanger. Then, the permeate is cooled to a temperature of 320ºC in the economizer and is supplied by the fan as an oxidant to the boiler`s combustion chamber. The air drawn to the ASU is compressed and then heated to a temperature of 750ºC in permeate-air heat exchanger. Then, the air flows to the separation membrane (feed) where the oxygen is separated. The gas leaving the membrane, that consists mostly of nitrogen, is called retentate. The retentate enters the expander and then is cooled by a feed water in the steam cycle. Expander drives the air compressor, and the excess of the mechanical power is used to generate electricity.

The paper includes the analysis and comparison with a classic gas turbine of an air separation unit

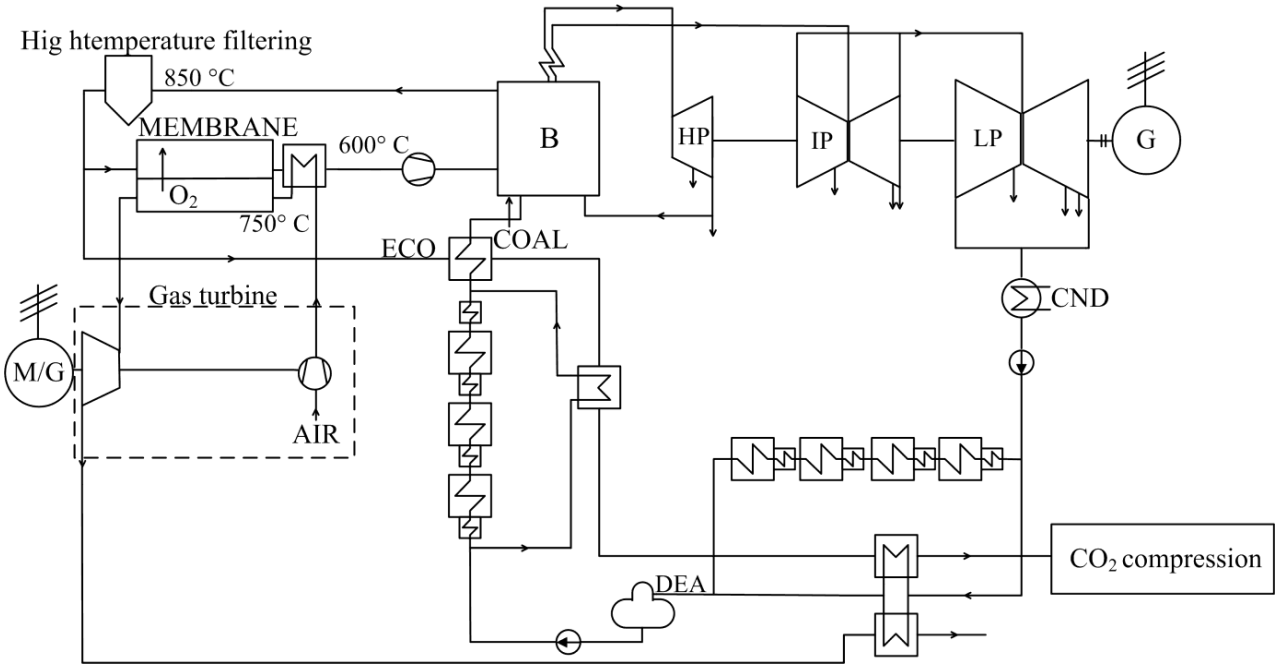

Fig. 1. Solution diagram of "four end", average integration [9]

(ASU). The computations results obtained with ASU model were compared with the results obtained using an autonomous gas turbine model. The air separation model will be used to build the models of oxy-combustion power plants.

Model of the air separation unit (ASU) and assumptions for calculations

Air separation unit structure consists of: counter-flow air heater (APH), air compressor (C), expander (EX), electric generator (G) and "four--end" type membrane (M). The expander drives the air compressor. Depending on the assumed quantities the expander and compressor can give or take electricity from the grid. The structure of the air separation unit is shown in figure 2. The characteristic basic quantities of the air separation unit and autonomous gas turbine are gathered in table 1.

It was assumed for the calculations that the air taken from environment is a dry gas consisting of 21% oxygen and 79% nitrogen (volumetric composition).

The characteristic quantities gathered in table 1 were used for computations performed on a "four-end" membrane air separation unit model, made in GateCycle™ software. The built-in components were used to build the air separation unit model. The quantity that determinates the value of the mass flow rate in the entire ASU model is a mass flow rate of oxygen. This mass flow rate is approximately the same as the oxygen mass flow rate feeding an oxy boiler working in a 460 MW power plant. It was assumed that through the membrane flows pure oxygen.

Table 1. Characteristic quantities for investigated air separation unit (ASU)

Name	Symbol	Value	Unit
Ambient pressure	p_{ot}	101.3	kPa
Ambient temperature	t_{ot}	20	ºC
Membrane working temperature	t_{mem}	750; 850	ºC
Stream of separated oxygen	$\dot{m}_{O2}$	107.56	kg/s
Oxygen recovery rate	R	40÷100	%
Compressor pressure ratio	β_K	2÷30	–
Compressor isentropic efficiency	η_{iS}	0.88	–
Expander isentropic efficiency	η_{iT}	0.9	–
Generator efficiency	η_g	0.99	–

The structure of an autonomous gas turbine as opposed to a structure of ASU shown in figure 2 does not contain a "four-end" type membrane. In the autonomous gas turbine model the assumption concerning a compressor, expander and air heater are the same as in the ASU model. The air mass flow rate in both models are the same, the difference is only in the mass flow rate and composition of gas flowing into the expander. In the ASU model the composition and mass flow rate of the gas is different from air because some oxygen is separated from air in the membrane. In the autonomous gas turbine model the mass flow rate and composition of gas flowing into the expander is the same as mass flow rate and composition of air leaving the air heater.

The results of calculations of air separation unit and autonomous gas turbine

The air mass flow rate depends on the separated in membrane oxygen mass flow rate ($\dot{m}_{O2}$), oxygen

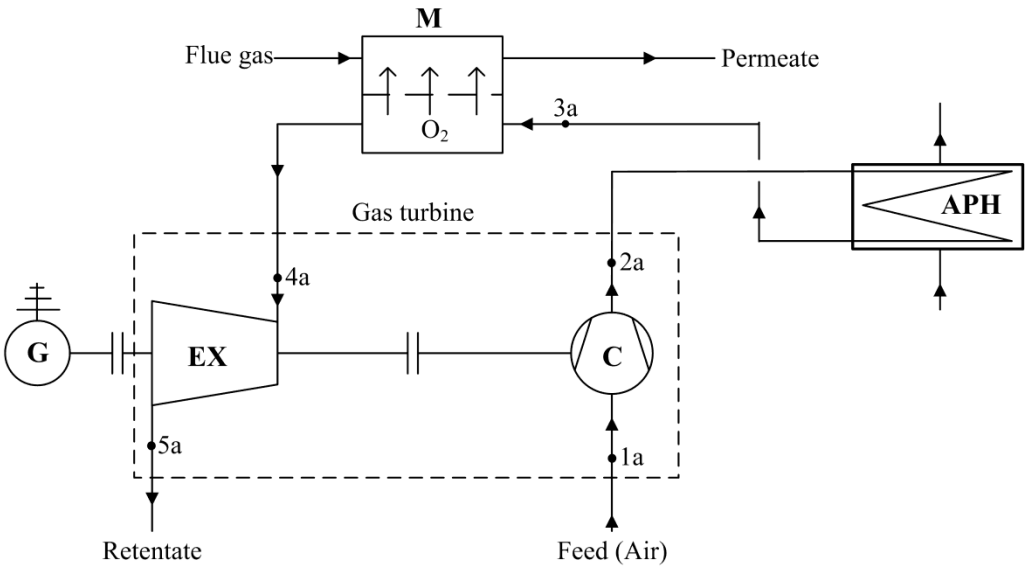

Fig. 2. Scheme of the air separation unit with gas turbine (ASU)

recovery rate (R) and mass content of oxygen in the air (g_{O2-air}). The relation between these quantities is as follows:

$$\dot{m}_{1a} = \frac{\dot{m}_{O2}}{R\, g_{O2-air}} \tag{2}$$

Next, the air is compressed by the compressor. Effective power required to drive the compressor depends on the air mass flow rate ($\dot{m}_{1a}$), the air temperature (T_{1a}), the average specific heat ($(\tilde{c}_p)_K$), the compressor pressure ratio (β_K), the heat capacity ratio contained in the factor ($\mu_K = ((\chi - 1)/\chi)_K$), the compressor isentropic efficiency (η_{iK}) and the compressor mechanical efficiency (η_{mK}). The equation showing the relation between these quantities is as follows:

$$N_{eK} = \dot{m}_{1a} (\tilde{c}_p)_K T_{1a} \left(\frac{\beta_K{}^{\mu_K} - 1}{\eta_{iK} \eta_{mK}} \right) \tag{3}$$

The mass flow rate flowing through the expander is lower than the oxygen mass flow rate separated in the membrane by the mass flow rate flowing through the compressor. This mass flow rate depends on the oxygen mass flow rate separated from the air in the membrane ($\dot{m}_{O2}$) and the air flow rate ($\dot{m}_{1a}$). The relation between these quantities is as follows:

$$\dot{m}_{4a} = \dot{m}_{1a} - \dot{m}_{O2} \tag{4}$$

The expander effective power depends on the retentate mass flow rate ($\dot{m}_{4a}$), the retentate temperature (T_{4a}), the average specific heat ($(\tilde{c}_p)_K$), the compressor pressure ratio (β_K), the reduction factor of compressor pressure ratio (σ), the heat capacity ratio contained in the factor ($\mu_T = ((\chi - 1)/\chi)_T$), the expander isentropic efficiency (η_{iT}) and the expander mechanical efficiency (η_{mT}). The equation showing the relation between these quantities is as follows:

$$N_{eT} = \dot{m}_{4a} (\tilde{c}_p)_T T_{4a} \left[1 - (\sigma \beta_K)^{-\mu_T} \right] \eta_{iT}\, \eta_{mT} \tag{5}$$

Figure 3 shows computed gross electric power as a function of oxygen recovery rate. The curve in this figure is determined for $\beta_K = 20$ and $t_{3a} = 750$ºC. The gross electrical power depends on the expander gross power (N_{eT}), the compressor gross power (N_{eK}) and the generator efficiency (η_g). The relation between these quantities is as follows:

$$N_{elTG} = (N_{eT} - N_{eK}) \eta_g \tag{6}$$

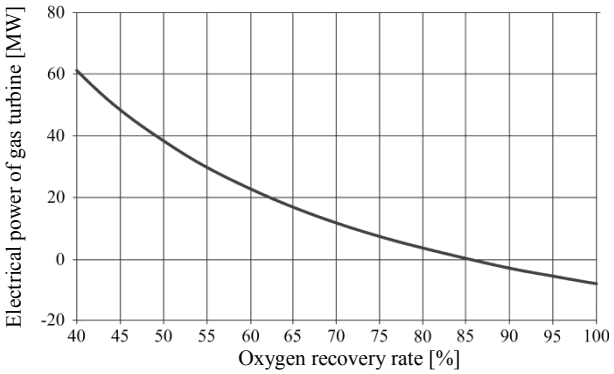

Fig. 3. Electrical power achieved or required for power the turbine set in ASU model as a function of oxygen recovery rate for $\beta_K = 20$ and $t_{3a} = 750$ºC

Figure 4 shows a graph of the electric power generation efficiency for $\beta_K = 20$ and $t_{3a} = 750$ºC. This efficiency depends on the gross electrical power (N_{elTG}) and the heat supplied to the unit (Q_d). The relation between these quantities is as follows:

$$\eta_{el} = \frac{N_{elTG}}{Q_d} \tag{7}$$

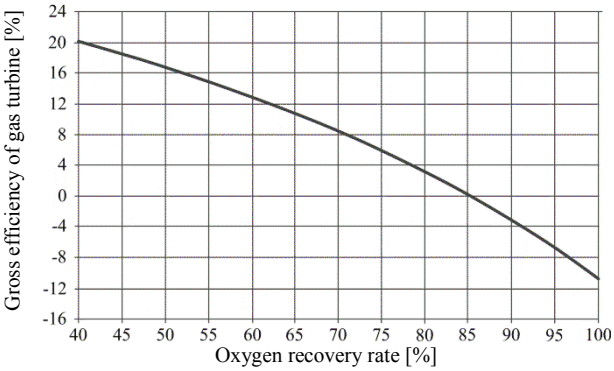

Fig. 4. Gross efficiency of ASU model as a function of oxygen recovery rate for $\beta_K = 20$ and $t_{3a} = 750$ºC

The heat supplied to the unit depends on the air mass flow rate ($\dot{m}_{2a}$), the air enthalpy (h_{2a}), the retentate mass flow rate ($\dot{m}_{4a}$) and retentate enthalpy (h_{4a}). The relation between these quantities is as follows:

$$Q_d = \dot{m}_{4a} h_{4a} - \dot{m}_{2a} h_{2a} \tag{8}$$

It should be noted that the gross electrical power (Fig. 3) at a large oxygen recovery rate is below zero. Equation for the maximal oxygen recovery rate using (2) and (5) is as follows:

$$R_{gr} \le \frac{1}{g_{O2}} \left[1 - \frac{T_{1a}}{T_{3a}} \frac{1}{\eta_{iK} \eta_{iT} \eta_{mK} \eta_{mT}} \frac{(\tilde{c}_p)_K}{(\tilde{c}_p)_T} \frac{\beta_K{}^{\mu_K} - 1}{1 - (\sigma \beta_K)^{-\mu_T}} \right] \tag{9}$$

Figure 5 shows graph of maximal oxygen recovery rate as a function of a compressor pressure ratio. Computations made for this graph were carried out with the use of GateCycle™ software for the two different membrane working temperature (t_{3a} = 750ºC and t_{3a} = 850ºC).

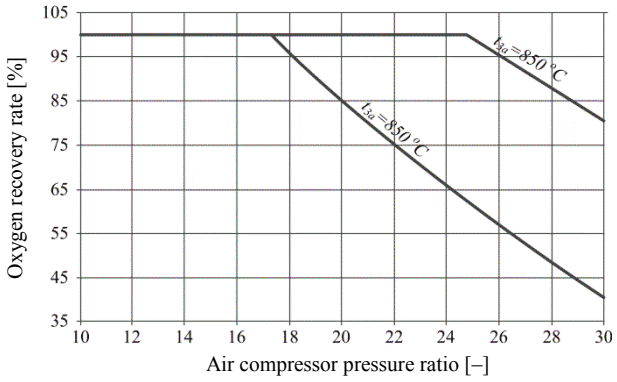

Fig. 5. Maximal oxygen recovery rate in the ASU model as a function of the compressor pressure rate for two different membrane work temperature

Figure 6 shows a graph of gross electric power of the air separation unit (marked as "ASU" on a graph) as a function of the compressor pressure ratio for the two different oxygen recovery rate (50% and 90%). The same figure also shows the gross electric power of the autonomous gas turbine (marked as "TG" on graph) as a function of the compressor pressure ratio for the same oxygen recovery rate.

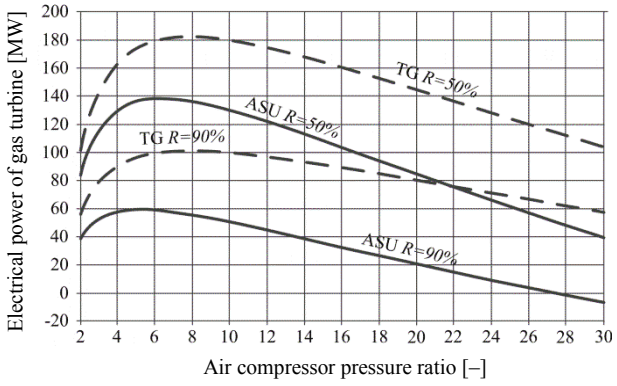

Fig. 6. Gross electrical power for both units as a function of compressor pressure ratio for two different oxygen recovery rate

It should be noted that the optimal compressor pressure ratio in the air separation unit and the autonomous gas turbine are not equal. Using (3) and (5) the optimal compressor pressure ratio in air separation unit can easily be determined:

$$\beta_{\mathrm{K}}^{\mathrm{opt(N_{eTG})}} = \left[\beta_{\mathrm{K}}^{\mathrm{opt(N_{eTG})}}\right]_{\mathrm{kl}} \left(1 - g_{\mathrm{O2}} R\right)^{\frac{1}{\mu_{\mathrm{K}}+\mu_{\mathrm{T}}}} \quad (10)$$

In the (8) optimal compressor pressure ratio ($\left[\beta_{\mathrm{K}}^{\mathrm{opt(N_{eTG})}}\right]_{\mathrm{kl}}$) is determined in the same way as for a classic gas turbine. Calculated optimal compressor pressure ratio values, due to generated electricity from the turbine set are gathered in table 2.

Table 2. The optimal compressor pressure ratio values, due to generated electricity from turbine set

Name	Symbol	Value		
Oxygen recovery rate	R [%]	50	70	90
Optimal compressor pressure ratio for ASU	$\beta_{\mathrm{K\_ASUopt}}$ [–]	6.4	5.8	5.3
Optimal compressor pressure ratio for TG	$\beta_{\mathrm{K\_TGopt}}$ [–]	7.8	7.8	7.8

The optimal compressor pressure ratio values, due to the gross efficiency, as well as for the autonomous gas turbine depends on the optimal compressor pressure ratio values, due to electricity generated from the turbine set ($\beta_{\mathrm{K}}^{\mathrm{opt(N_{eTG})}}$) and the gross efficiency of the electricity generation of the unit (η_{elTG}). The relation between these quantities is as follows:

$$\beta_{\mathrm{K}}^{\mathrm{opt(\eta_{eTG})}} = \beta_{\mathrm{K}}^{\mathrm{opt(N_{eTG})}} \left(\frac{1}{1-\eta_{\mathrm{elTG}}\eta_{\mathrm{mK}}}\right)^{\frac{1}{\mu_{\mathrm{K}}+\mu_{\mathrm{T}}}} \quad (11)$$

Equation (11) was determined using (3), (5) and (7), with the condition $\mathrm{d}\eta_{\mathrm{elTG}} / \mathrm{d}\beta_{\mathrm{K}} = 0$.

Figure 7 shows a graph of gross efficiency of electricity generation as a function of the compressor pressure ratio for the two different oxygen recovery rates in the air separation unit (50% and 90%) and for autonomous gas turbine.

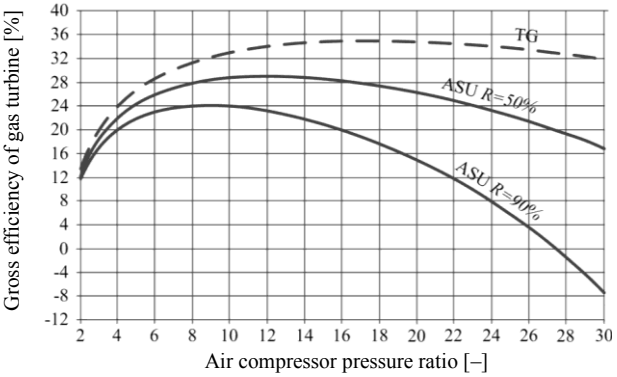

Fig. 7. Gross efficiency of both units as a function of compressor pressure ratio for two different oxygen recovery rate

Calculated optimal compressor pressure ratio values, due to the gross efficiency are gathered in table 3.

Table 3. The optimal compressor pressure ratio values, due to gross efficiency of both units

Name	Symbol	Value		
Oxygen recovery rate	R [%]	50	70	90
Optimal compressor pressure ratio for ASU	β_{K_ASUopt} [–]	11.9	10.2	8.8
Optimal compressor pressure ratio for TG	β_{K_TGopt} [–]	17.6	17.6	17.6

Conclusions

In this paper the air separation unit with "four--end" high-temperature membrane (HTM) was analyzed.

For the analysis of the air separation unit and of the autonomous gas turbine power and efficiency characteristic as a function of oxygen recovery rate and compressor pressure ratio were determined. The characteristics for both units are summarized and compared in the figures 6 and 7.

The maximal oxygen recovery rate as a function of the compressor pressure ratio for the two different membrane work temperature were determined. This quantity separates the area of work in which we get the extra power from expander in the air separation unit from the area of work in which we must deliver additional power to drive the compressor.

The optimal compressors pressure ratio due to a power of turbine set and due to the efficiency of electricity generation for different oxygen recovery rates in the air separation unit and in the autonomous gas turbine were determined. The optimal values of compressor pressure ratio in the air separation unit are decreasing with the increase of the oxygen recovery rate. In the case of the autonomous gas turbine, these values are constant.

Acknowledgements

The results presented in this paper were obtained from research work co-financed by the National Centre for Research and Development within a framework of Contract SP/E/2/66420/10 – Strategic Research Programme – Advanced Technologies for Energy Generation: Development of a technology for oxy-combustion pulverized-fuel and fluid boilers integrated with CO_2 capture.

References

1. CHMIELNIAK T.: The role of various technologies in achieving emissions objectives in the perspective of the years up to 2050. Rynek Energii, 2011, 1 (92), 3–9.
2. CHMIELNIAK T., ŁUKOWICZ H., KOCHANIEWICZ A.: Trends of modern power units efficiency growth. Rynek Energii, 2008, 6 (79), 14–20.
3. KOTOWICZ J., JANUSZ-SZYMAŃSKA K.: Influence of CO_2 separation on the efficiency of the supercritical coal fired power plant. Rynek Energii, 2011, 2 (93), 8–12.
4. LISZKA M., ZIĘBIK A.: Coal – fired oxy – fuel power unit – Process and system analysis. Energy, 35 (2010), 943–951.
5. TOFTEGAARD M.B., BRIX J., JENSEN P.A., GLARBORG P., JENSEN A.D.: Oxy-fuel combustion of solid fuels. Progress in Energy and Combustion Science, 2010, 36, 581–625.
6. DILLON D.J., WHITE V., ALLAM R.J., WALL R.A., GIBBINS J.: Oxy-combustion Process for CO_2 Capture from Power Plant. Mitsui Babcock Energy Limited, 2005.
7. BUHRE B.J.P., ELLIOTT L.K., SHENG C.D., GUPTA R.P., WALL T.F.: Oxy-fuel combustion technology for coal-fired power generation. Progress in Energy and Combustion Science, 2005, 31, 283–307.
8. PFAFF I., KATHER A.: Comparative thermodynamic analysis and integration issues of CCS steam power plants based on oxy-combustion with cryogenic or membrane based air separation. Energy Procedia, 1 (2009), 495–502.
9. STADLER H. et al.: Oxyfuel coal combustion by efficient integration of oxygen transport membranes. International Journal of Greenhouse Gas Control, 5 (2011), 7–15.